

Characterizing the dynamics of coupled pendulums via symbolic time series analysis

G. De Polsi^{1,a}, C. Cabeza¹, A.C. Martí¹, and C. Masoller²

¹ Instituto de Física, Universidad de la República, Iguá 4225, Montevideo 11400, Uruguay

² Departament de Física i Enginyeria Nuclear, Universitat Politècnica de Catalunya,
Colom 11, 08222 Terrassa, Barcelona, Spain

Received 27 March 2013 / Received in final form 25 April 2013

Published online 25 June 2013

Abstract. We propose a novel method of symbolic time-series analysis aimed at characterizing the regular or chaotic dynamics of coupled oscillators. The method is applied to two identical pendulums mounted on a frictionless platform, resembling Huygens' clocks. Employing a transformation rule inspired in ordinal analysis [C. Bandt and B. Pompe, Phys. Rev. Lett. **88**, 174102 (2002)], the dynamics of the coupled system is represented by a sequence of symbols that are determined by the order in which the trajectory of each pendulum intersects an appropriately chosen hyperplane in the phase space. For two coupled pendulums we use four symbols corresponding to the crossings of the vertical axis (at the bottom equilibrium point), either clock-wise or anti-clock wise. The complexity of the motion, quantified in terms of the entropy of the symbolic sequence, is compared with the degree of chaos, quantified in terms of the largest Lyapunov exponent. We demonstrate that the symbolic entropy sheds light into the large variety of different periodic and chaotic motions, with different types synchronization, that cannot be inferred from the Lyapunov analysis.

1 Introduction

Ordinal analysis is a well-known tool for the analysis of complex systems [1] that has allowed to identify novel features in the dynamics of such systems, as for example the existence of forbidden patterns [2–4]. Originally proposed by Bandt and Pompe [5], the method has been widely employed for time-series analysis (predictability, similarity, coupling directionality, classification, etc.) [6–12] of discrete-time dynamical systems, and of continuous-time systems, at an event-level description (i.e., in terms of events as neuronal spikes). By applying cross recurrence plots, ordinal analysis was also successfully used to visualize dependencies between two time series and to measure the synchronization degree of coupled oscillators [13]. More recently, from an algebraic perspective, ordinal patterns was employed to investigate the synchronization regimes of chaotic oscillators [14,15].

^a e-mail: gdepolsi@fisica.edu.uy

In this work we consider as a paradigmatic toy model, inspired in famous Huygens' pendulum clocks [16–21], two identical pendulums mounted on a frictionless platform. When the system evolves in a vertical plane, the state of each pendulum is described by two variables: the angle with the vertical direction, and its time derivative; and the motion of the common platform is also described by two variables: the linear displacement and its time derivative. Thus, the time evolution of the coupled system occurs in a six-dimensional phase space. Assuming that the total energy and the linear momentum are conserved, then the phase space can be reduced to a four-dimensional one. However, by studying the projection of the trajectory in lower, two or three dimensional phase spaces, is difficult to extract information useful for identifying the different types of regular or chaotic motions of the two pendulums.

Inspired by ordinal analysis, here we propose a novel symbolic method for describing the motion of coupled oscillators, at an event-level description, and apply the method to the specific case of the coupled pendulums. We consider the evolution of the system in the center of mass reference frame, and consider the crossings of each pendulum of the vertical axis at the bottom equilibrium point. Then, these events can be represented as a symbolic sequence using the following rule: when the crossing of pendulum 1 (pendulum 2) is clock-wise, is represented by symbol A (B), and when is anti-clock-wise, is represented by symbol C (D). Thus, this transformation rule allows to describe the complex motion of the two pendulums in the four-dimensional phase space by a sequence of symbols (or letters), each having 4 possible values. This method can be easily extended to a larger number of coupled oscillators, or to a more detailed description of the dynamics (by considering the crossings with other hyper-planes as additional events to be represented by other symbols).

To characterize the dynamics of the system we compute the largest Lyapunov exponent of the full model equations (in the following referred to as LLE), and the Shannon entropy of the symbolic sequence (in the following referred to as symbolic Shannon entropy, SSE). To compute the SSE the symbolic sequence is transformed into a sequence of patterns (or words), formed by L consecutive symbols (or letters), and compute the probabilities of all the possible patterns, following the same procedure as in ordinal analysis. For example, with four symbols representing “clock-wise” and “anti-clock-wise” vertical crossings of pendulums 1 and 2, there are 4^L different words of L letters.

The outline of this paper is as follows. In Sec. 2 the formalism of the SSE is presented and applied to the system of coupled pendulums described in Sec. 3. Section 4 presents the numerical results and discusses the different types of motion identified in terms of their entropy and Lyapunov values. Using the total energy of the system as the control parameter we demonstrate that the SSE is capable of capturing different types of rhythmic oscillations, including *in phase and anti phase* motions of the two pendulums, thus providing important information that could not be inferred from the calculation of the LLE. Finally, Sec. 5 presents a summary of the results and the conclusions.

2 Symbolic analysis of coupled pendulums

Most conservative systems may exhibit, depending on the initial conditions and the parameters, regular or chaotic dynamics. Several methods have been proposed to characterize the dynamics of such systems including Lyapunov exponents, power spectra and Poincaré sections [22]. Here we consider a system composed by two ideal pendulums mounted in a platform. A symbolic sequence is obtained from the time-evolution of the system by considering the intersections of the trajectories in the phase space with adequately defined hyperplanes. Every time one of the pendulums crosses

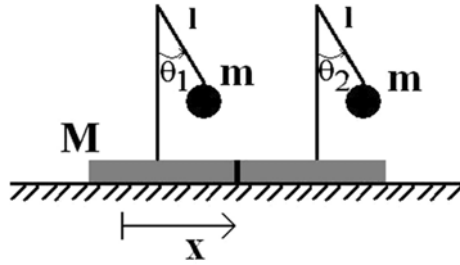


Fig. 1. Schematic representation of two identical pendulums mounted on a frictionless platform.

an hyperplane we assign a symbol according to which pendulum crosses, 1 or 2, and in which direction. Specifically, letter A (C) corresponds to pendulum 1 crossing the bottom equilibrium point with positive (negative) angular velocity and B (D), to pendulum 2 crossing with positive (negative) angular velocity. In this way we obtain, from the motion of the coupled pendulums, a sequence of symbols, e.g. $A,B,C,D,A,B,C,D\dots$

Next, the sequence of N symbols is transformed into a sequence of $M = N/L$ patterns (or words) by dividing the sequence of symbols into non-overlapping sets of L consecutive symbols. For example, with $L = 4$ there are 4^L possible words: $AAAA,AAAB,AAAC,\dots$; however, many of these might be forbidden by the conservation laws of energy and momentum. Then, the probability of each word, p_i with $i = 1 \dots 4^L$, is computed from the number of appearances of each word in the sequence of words, and finally, with these probabilities the symbolic Shannon entropy (SSE) is calculated as $S = -\sum_i p_i \ln p_i$.

The symbolic entropy measures the degree of the disorder of the motion of the system, as a regular motion will have an ordered sequence of symbols (thus, only few words will appear in the sequence of words), giving a low SSE value. On the contrary, a chaotic motion can be expected to have a disordered sequence of symbols, which will result in a sequence of words where more words (or even all possible words) appear, and these can be expected to have more widely distributed probabilities, and as a consequence, a larger value of the SSE.

We remark that this method of symbolic analysis is quite general and can be extended both, to higher dimensional systems (e.g., to a larger number of oscillators) and to more than two hyper-planes. For example, by considering also the crossings of the top (unstable) equilibrium point we could have a more detailed (event-level) description of the motion.

3 Model equations

We consider two identical pendulums, of mass m and length l , mounted on a frictionless platform of mass M , as shown schematically in Fig. 1. The coupling between the pendulums comes from the common platform. The generalized coordinates are chosen as the angles θ_1 and θ_2 and the position of the platform x . The equations of motion can be readily obtained from the Lagrangian of the system [23]

$$L = \left(\frac{M}{2} + m\right)\dot{x}^2 + \frac{ml^2}{2}(\dot{\theta}_1^2 + \dot{\theta}_2^2) + ml\dot{x}\left[\dot{\theta}_2 \cos \theta_1 + \dot{\theta}_1 \cos \theta_2\right] + mgl(\cos \theta_1 + \cos \theta_2). \quad (1)$$

Due to the fact that the system is invariant under horizontal translations, the x coordinate is cyclic and can be eliminated from the equations of motion. In this way

we obtain a system of two ordinary differential equations for the angular variables of the pendulums

$$\begin{aligned}\ddot{\theta}_1 + \frac{g}{l} \sin \theta_1 &= \frac{m}{M+2m} (\ddot{\theta}_1 \cos \theta_1 - \dot{\theta}_1^2 \sin \theta_1 + \ddot{\theta}_2 \cos \theta_2 - \dot{\theta}_2^2 \sin \theta_2) \\ \ddot{\theta}_2 + \frac{g}{l} \sin \theta_2 &= \frac{m}{M+2m} (\ddot{\theta}_2 \cos \theta_2 - \dot{\theta}_2^2 \sin \theta_2 + \ddot{\theta}_1 \cos \theta_1 - \dot{\theta}_1^2 \sin \theta_1),\end{aligned}\quad (2)$$

which can be related to the position of the platform using the expression for the momentum along the x -direction

$$p_x = \left(\frac{M}{2} + m\right)\dot{x} + ml(\dot{\theta}_2 \cos \theta_1 + \dot{\theta}_1 \cos \theta_2) = \text{constant}. \quad (3)$$

In addition to the conservation of p_x , the energy is also conserved. However, instead of using the conservation of the energy to reduce the phase-space of the system, we use this magnitude to ensure the exactness of the numerical integration method (the equations are integrated with a 5-th order Runge-Kutta method with variable step-size to guarantee the conservation of the energy up to 10^{-5}). The initial conditions are chosen with p_x and the angles of both pendulums equal zero. Thus, the motion of the system is determined by its energy and by the initial velocity of one of the pendulums. We consider as control parameters the reduced energy, $E^* = E/((M+2m)l)$, and the initial angular velocity of pendulum 1, $(d\theta_1/dt)_0$. These quantities are not independent and for a given value of E^* , only an interval of values of $(d\theta_1/dt)_0$ is possible. Thus, physically meaningful initial conditions are located inside a parabola in the parameter space $(E^*, (d\theta_1/dt)_0)$.

4 Numerical results

In this section we present the results of the numerical simulations. The parameters are $M/m = 3$ and $l = 0.1\text{m}$, $g = 9.8\text{m/s}^2$ and the simulation time is at least 100s. The SSE is calculated, as explained in Sec. 2, with events (A, B, C, D) defined by the crossing of the pendulums with the bottom equilibrium point in each direction and forming words of $L = 4$. Depending on the region of the parameter space, the number of letters obtained from the trajectories for computing the probabilities are 6000 or 8000.

Figure 2 displays in color code the value of the symbolic entropy for each set of initial conditions for words of $L = 3$ (right panel) and $L = 4$ (left panel). It can be observed that in both cases the SSE shows an overall trend to increase with the energy: for low energies, low values of the SSE (indicated in blue and yellow tones) prevail, while for high energies, the SSE increases (in red). In relation to the comparison between both panels (for easier comparison they are done with the same color scale), we observe that in the region of small oscillations the $L = 3$ entropy is actually larger than the $L = 4$ entropy. This is due to the fact that, for two pendulums, a word with an even number of letters is more suitable to accommodate the normal modes of oscillation of the pendulums. In the opposite limit of high energies and chaotic trajectories there are no significant differences and for high entropy values, the $L = 3$ and $L = 4$ symbolic entropies are almost linearly related (as shown in Fig. 4(b)).

Figure 3(a) displays the largest Lyapunov exponent corresponding to the same trajectory (i.e., the same initial conditions) as Fig. 2. Comparing Fig. 2 and Fig. 3(a) one observes that the SSE reproduces the same structure of the LLE, distinguishing chaotic and non-chaotic behaviors. However, in addition, in the regions of regular motion where the LLE is zero (dark blue in Fig. 3(a)), the SSE displays a broad range of values, corresponding to different types of regular motions.

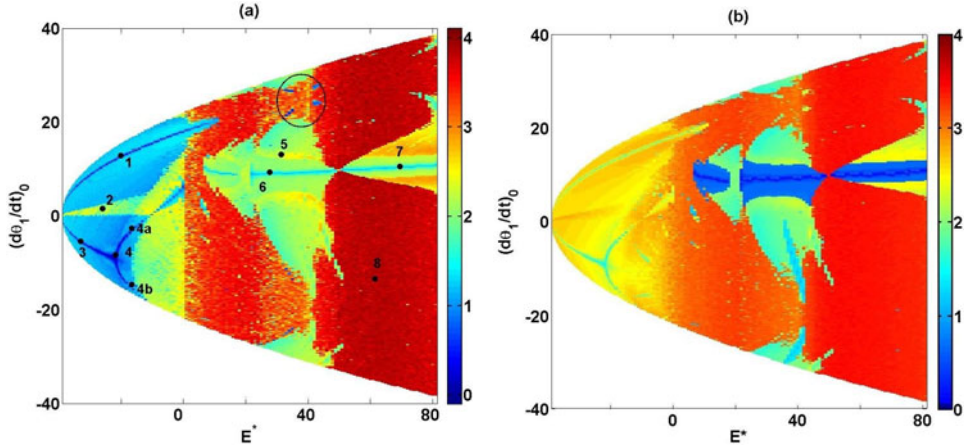


Fig. 2. Symbolic entropy as a function of the reduced energy and the initial angular velocity of pendulum 1 for $L = 4$ (a) and $L = 3$ (b). The labels and the circle indicate points or regions whose dynamics is discussed in the text.

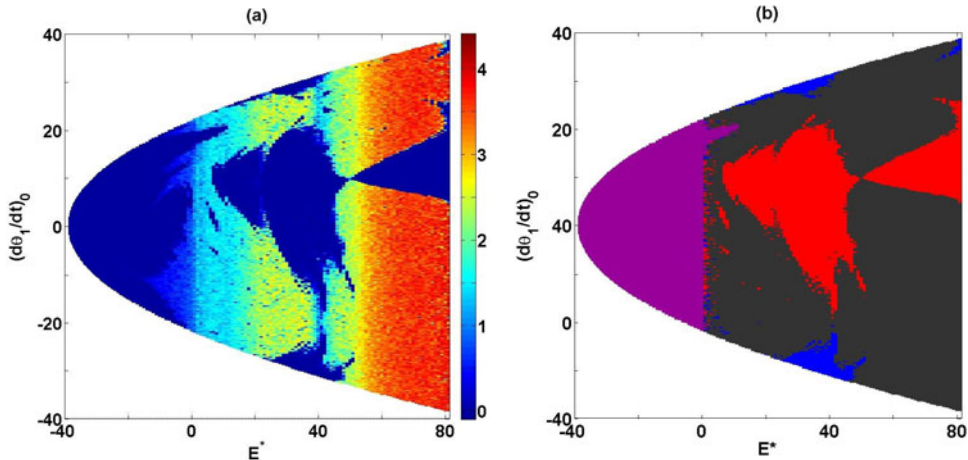


Fig. 3. (a) Largest Lyapunov exponent in color-code as a function of the reduced energy and the initial angular velocity of pendulum 1. (b) Rotating motion of the two pendulums: purple represents motions in which neither of the two pendulums spins around; red and blue represent motions in which only one pendulum spins around, and black represents motions in which both pendulums spin around.

To gain insight into the dynamics, Fig. 3(b) displays in color code the behavior of the pendulums: purple represents motions in which neither of the two pendulums spins around (i.e., θ_1 and θ_2 are both confined to some interval of values); red and blue represent motions in which only one pendulum spins around (i.e., either θ_1 or θ_2 is confined to some interval of values), and black represents motions in which both pendulums spin around (i.e., neither θ_1 or θ_2 is confined).

The clear border at $E^* = 1.4$ observed in plot of the symbolic entropy, Fig. 2, and also seen in the plot of the largest Lyapunov exponent, Fig. 3(a), can be understood when observing the spinning behavior of the two pendulums displayed in Fig. 3(b): the regions of low SSE and LLE can be identified with motions in which none or only one of the pendulums spins around.

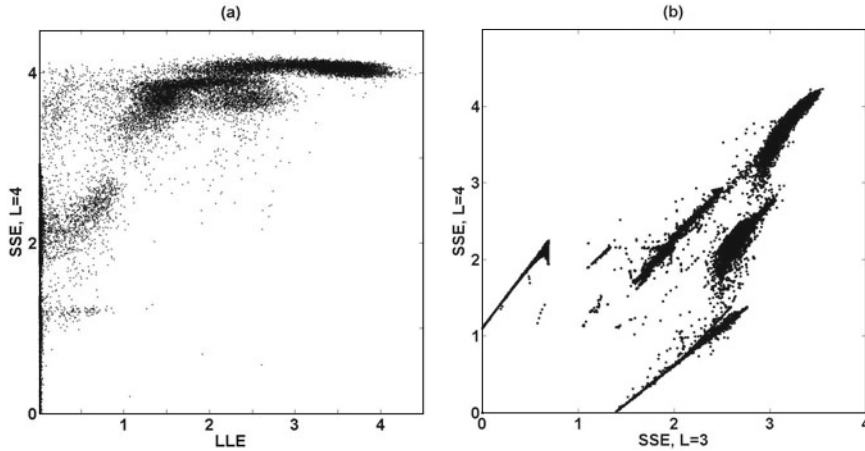


Fig. 4. Symbolic Shannon entropy vs. the largest Lyapunov exponent (a) and SSE with $L = 3$ vs. $L = 4$ (b) for all the initial conditions considered in Figs. 2 and 3.

A nonlinear relation between the symbolic entropy and the largest Lyapunov exponent can be appreciated in Fig. 4. In this figure, the value of the SSE is plotted vs the value of the LLE, for all the initial conditions considered in Figs. 2 and 3. It can be observed that for zero and for low values of the LLE (corresponding to regular or weakly chaotic motion), there is a range of possible values of the SSE that distinguishes the degree of regularity of the motion; notice however that all these values are lower than the SSE values that correspond to chaotic behavior: while regular (or weakly chaotic) motions have SSE lower than 3, chaotic motions tend to have SSE close to 4.

Let us now analyze the motion of the two pendulums at some specific initial conditions using the SSE diagram. We refer to the points as labeled in Fig. 2. In this figure, at low SSE values, two clear curves can be seen, in dark blue, starting at the vertex of the parabola. Along these curves the two pendulum oscillate with equal amplitude and frequency, *in phase* in the upper curve and *anti phase* in the lower curve. Figure 5 displays a few examples of the temporal evolution of the angular variables. In point 1 (*in phase* motion), and in point 3 (*anti phase* motion) the pendulums oscillate with nearly the same amplitude. Points 2 and 6 also correspond to *in phase* motions; the value of the SSE is larger for point 2 than in points 1 and 3 because of the higher number of frequencies present in the spectrum, but still low enough in comparison with a chaotic motion. Note, that in contrast to points 1, 3, and 6, point 2 presents a superposition of the different frequencies resulting in the typical pattern of a beat.

The curve in light blue of low SSE values where points 6 and 7 are located corresponds to *in-phase* synchronization with a relation of frequencies (1 : 1). However, along this curve, not only the oscillation amplitude of the pendulums is different, but also, one pendulum spins around and the other does not (the dynamics in point 6 is shown in Fig. 5). Although the (1 : 1) relation between the frequencies of the two pendulum is kept constant along the line joining points 6 and 7, the value of the frequency changes continuously.

Exploring other regions in Fig. 2 corresponding to larger SSE values we found that the more dissimilar the values of the amplitudes of the pendulums, the larger the value of the symbolic entropy.

The equal-amplitude *anti phase* curve starting at the vertex of the parabola in Fig. 2 bifurcates at point 4 forming two branches. The motion along those branches is still *anti phase*, however, in the upper branch the amplitude of pendulum 1 is larger

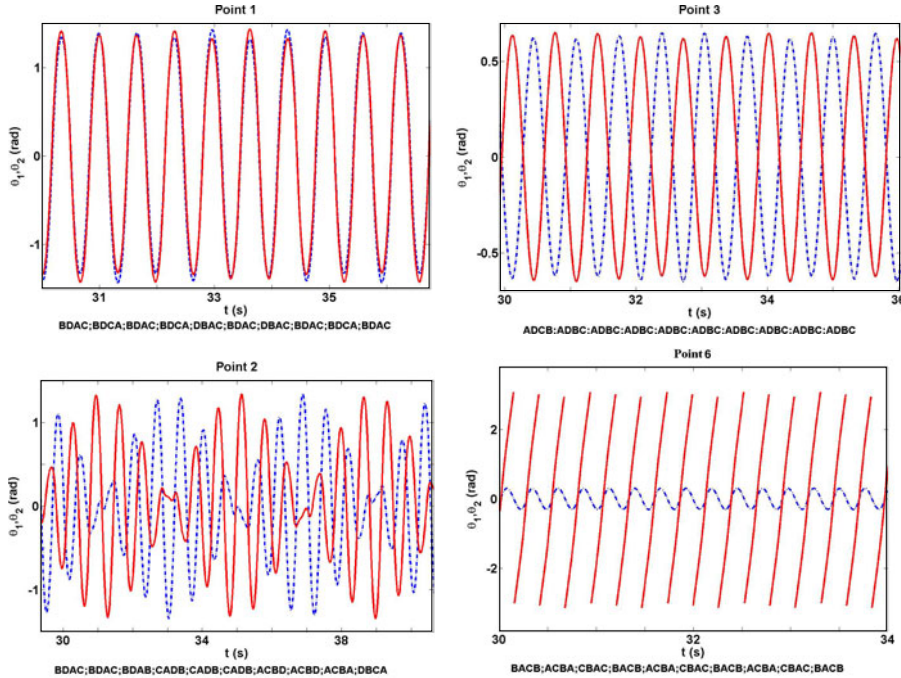


Fig. 5. Time evolution of the angular coordinates and the corresponding sequence of pattern of the two pendulums. Solid red (dashed blue) line corresponds to pendulum 1 (2). The initial conditions correspond to the points labeled 1, 3, 2, and 6 in Fig. 2. The value of the symbolic entropy is 1.1838 (point 1), 0.7207 (point 3), 2.2625 (point 2) and 1.2057 (point 6).

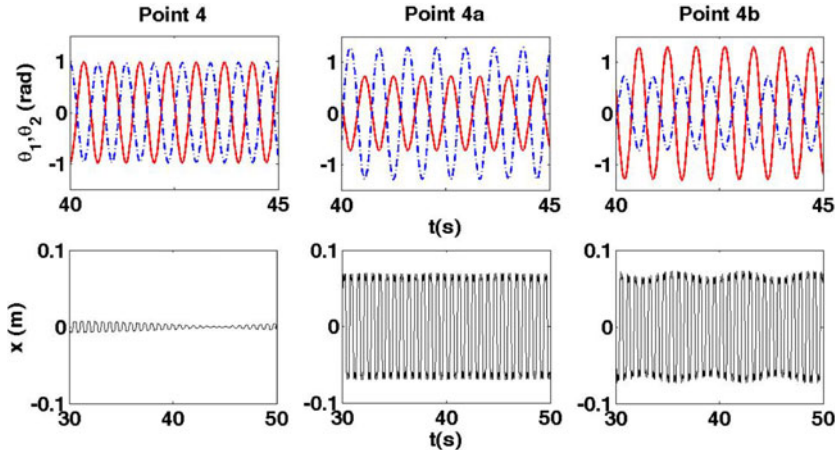


Fig. 6. Top row: temporal evolution of the angular variables of pendulum 1 (solid red line) and 2 (dashed blue line) for points 4, 4a, and 4b. Bottom row: temporal evolution of the platform position at the corresponding points. The value of the symbolic entropy is 0 (point 4), 0.0414 (point 4a) and 0.0447 (point 4b).

than that of pendulum 2, while in the lower branch the opposite situation occurs. It is worth noting that the amplitude of the oscillations of the platform is larger at points with different amplitudes in the angular variables, points 4a and 4b, than in the points with equal amplitude, for example, point 4. Figure 6 shows a comparison of the angular variables and the coordinate of the platform at points 4, 4a, and 4b.

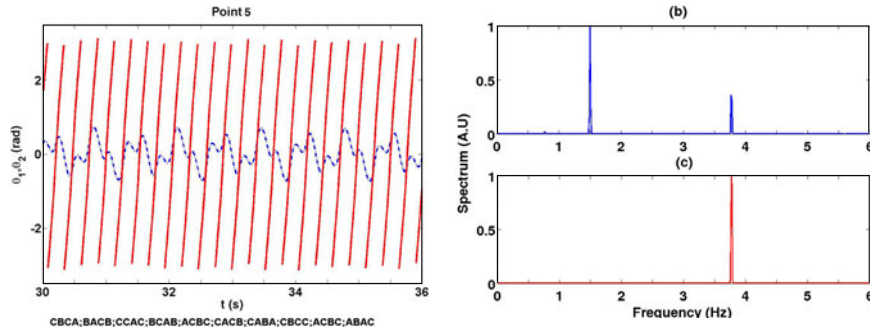


Fig. 7. Motion in point 5: angular variables [left, the solid red (dashed blue) line corresponds to pendulum 1 (2)] and their spectra [right, the top (bottom) panel corresponds to pendulum 1 (2)]. The value of the symbolic entropy is 2.5533.

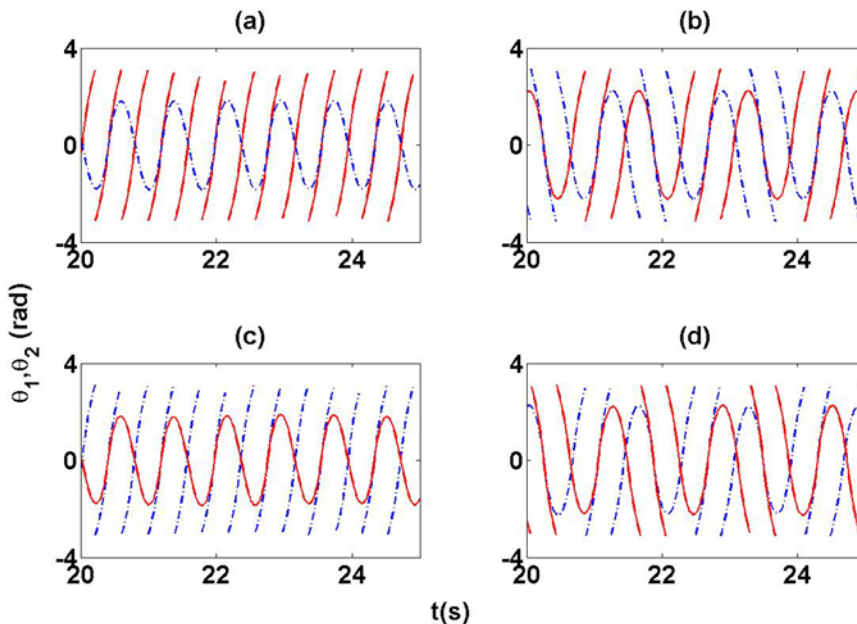


Fig. 8. Temporal evolution of the angular variables corresponding to initial conditions located inside the regions of regular dynamics enclosed in a circle in Fig. 2.

Another type of motion occurs for example in point labeled 5, displayed in Fig. 7. Here one can observe a form of locking of the frequencies of the two pendulums.

There are narrow isolated regions of regular motion at relatively high values of energy like the four small island enclosed in a circle in Fig. 2. Figure 8 shows the temporal evolution of the angular variables for points corresponding to each of the islands. In the two islands on the left, one of the pendulum is oscillating while the other is rotating and performs two complete turns for each period of the pendulum that oscillates. Concerning the islands on the right, the two pendulums alternate rotation and oscillation with the same period as depicted in Fig. 8.

For the sake of completeness, in Fig. 9 we show the dynamics of an initial condition corresponding to the fully chaotic region (point 8 in Fig. 2). In this dynamics the probabilities of the words are broadly distributed.

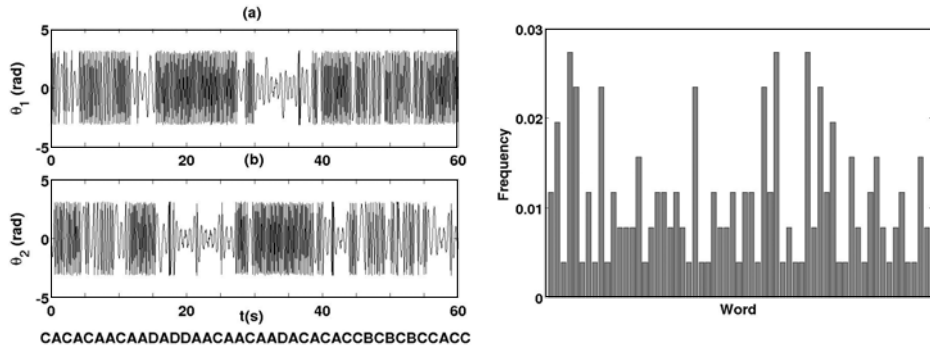


Fig. 9. Chaotic oscillation corresponding to point 8, where the value of the symbolic entropy is 3.9166. Left panels: angular variables of pendulum 1 (a) and pendulum 2 (b). Right panel: histogram of occurrences of the different words (only the words appearing in the time intervals on the left panels are plotted).

5 Conclusion

To summarize, we proposed a novel method of nonlinear time-series analysis, suitable for studying systems exhibiting regular or chaotic motion. The analysis is based on a symbolic transformation with rules that take into account the order of intersections of the trajectory with adequately defined hyper-planes in the phase space. The proposed formalism was applied to two identical pendulums mounted on a frictionless platform. The degree of complexity of motion was analyzed by computing the entropy of the symbolic sequence and by comparing with the largest Lyapunov exponent. We demonstrated that the symbolic entropy provides useful insight about specific features of the dynamics of coupled pendulums (in-phase and anti-phase motions, similar vs dissimilar amplitudes, frequency locking, etc.) that could not be inferred from the Lyapunov analysis. It would be interesting in the future to apply the proposed methodology for the analysis of the dynamics of non-identical pendulums and the influence of external forcing, noise and friction.

Due to its simplicity, this methodology can be applied to experimental data, as it only requires an event-level description of the dynamics (and does not require the knowledge of the details of the oscillations). Experimentally, it can be difficult to obtain long enough time series of the variables of a system, and our method only requires recording specific events as the crossing of the trajectory with suitable hyperplanes.

The methodology can be easily extended to account for an arbitrary number of oscillators and can therefore be very useful to study phenomena such as crowd-synchrony and quorum-sensing [24–27] that occur when a large enough number of oscillators interact with each other through a common medium (in our system, the frictionless platform).

We acknowledge financial support from Programa de Desarrollo de las Ciencias Basicas (PEDECIBA), and Comision Sectorial de Investigacion Cientifica (Universidad de la Republica, Uruguay). C. M. acknowledges partial support from the Spanish MCI (FIS2012-37655-C02-01), the Generalitat de Catalunya (2009 SGR 1168) and the ICREA Academia programme.

References

1. J.M. Amigo, *Permutation Complexity in Dynamical Systems: Ordinal Patterns, Permutation Entropy and All That* (Springer, Berlin, 2010)
2. J.M. Amigo, S. Zambrano, M.A.F. Sanjuan, EPL **79**, 50001 (2007)

3. K. Schindler, H. Gast, L. Stieglitz, et al., *Epilepsia* **52**, 1771 (2011)
4. M. Zanin, *Chaos* **18**, 013119 (2008)
5. C. Bandt, B. Pompe, *Phys. Rev. Lett.* **88**, 174102 (2002)
6. X. Li, G. Ouyang, D.A. Richards, *Epilepsy Res.* **77**, 70 (2007)
7. G. Ouyang, C. Dang, D.A. Richards, et al., *Clinical Neurophys.* **121**, 694 (2010)
8. A. Bahraminasab, F. Ghasemi, A. Stefanovska, P.V.E. McClintock, H. Kantz, *Phys. Rev. Lett.* **100**, 084101 (2008)
9. E. Olofsen, J.W. Sleigh, A. Dahan, *British J. Anaesthesia* **101**, 810 (2008)
10. U. Parlitz, S. Berg, S. Luther, A. Schirdewan, J. Kurths, N. Wessel, *Comp. Biolg. Med.* **42**, 319 (2012)
11. L. Zunino, M.C. Soriano, O.A. Rosso, *Phys. Rev. E* **86**, 046210 (2012)
12. M. Zanin, L. Zunino, O.A. Rosso, et al., *Entropy* **14**, 1553 (2012)
13. A. Groth, *Phys. Rev. E* **72**, 046220 (2005)
14. R. Monetti, W. Bunk, T. Aschenbrenner, F. Jamitzky, *Phys. Rev. E* **79**, 046207 (2009)
15. J.M. Amigo, R. Monetti, T. Aschenbrenner, W. Bunk, *Chaos* **22**, 013105 (2012)
16. M. Bennett, M.F. Schatz, H. Rockwood, K. Wiesenfield, *Proc. R. Soc. Lond. A Mat.* **458**, 563 (2002)
17. E. Klarreich, *Amer. Scient.* **90**, 322 (2002)
18. M. Rosenblum, A. Pikovsky, *Contemp. Phys.* **44**, 401 (2003)
19. R. Dilão, *Chaos* **19**, 023118 (2009)
20. H. Ulrichs, A. Mann, U. Parlitz, *Chaos* **19**, 043120 (2009)
21. M. Kapitaniak, K. Czolczynski, P. Perlikowski, A. Stefanski, T. Kapitaniak, *Phys. Rep.* **517**, 1 (2012)
22. A.J. Lichtenberg, M.A. Liberman, *Regular and Stochastic Motion: Applied Mathematical Sciences* (Springer-Verlag, Berlin, 1982)
23. H. Goldstein, C.P. Poole Jr., J.L. Safko, *Classical Mechanics* (Addison-Wesley, 1980)
24. S.H. Strogatz, D.M. Abrams, A. McRobie, B. Eckhardt, E. Ott, *Nature* **438**, 43 (2005)
25. S. De Monte, F. d'Ovidio, et al., *Proc. Natl. Acad. Sci. U.S.A.* **104**, 18377 (2007)
26. A.F. Taylor, M.R. Tinsley, F. Wang, Z. Huang, K. Showalter, *Science* **323**, 614 (2009)
27. J. Zamora-Munt, et al., *Phys. Rev. Lett.* **105**, 264101 (2010)